How does canal taper affect root stresses?

B. D. Rundquist[1] & A. Versluis[2]

[1]Restorative Sciences – Endodontics, School of Dentistry, University of Minnesota; and [2]Minnesota Dental Research Center for Biomaterials and Biomechanics, School of Dentistry, University of Minnesota, Minneapolis, MN, USA

Abstract

Rundquist BD, Versluis A. How does canal taper affect root stresses? *International Endodontic Journal*, **39**, 226–237, 2006.

Aim To examine the effect of specific tapers on root stresses and thus vertical root fracture.

Methodology The effect of taper on root stresses was calculated during simulated warm vertical compaction of gutta-percha in a straight rooted premolar for three tapers (0.04, 0.06 and 0.12 mm mm^{-1}) using finite element analysis. Stresses in the dentine were observed whilst the root was filled with three subsequent gutta-percha increments. Each increment was compacted at 10 or 15 N and the gutta-percha cooled down to 37 °C. After filling, composite was polymerized in the access space. A functional occlusal load of 50 N was then applied on the buccal cusp incline. The stress distribution in the root during the occlusal loading was compared with the stresses during filling.

Results During filling, the highest stresses were found: (a) at the canal surface; (b) using the smallest taper; (c) in the apical third; and (d) during the first gutta-percha increment. The root stress distribution changed when the functional post-filling load was applied. It generated the highest stresses at the external root surface, with a tensile stress concentration at the lingual surface of the cervical third. Since the stresses during simulated masticatory loading concentrated on the external surface, an increased taper size caused only slightly higher root stress levels.

Conclusions With increasing taper, root stresses decreased during root filling but tended to increase for masticatory loading. Root fracture originating at the apical third is likely initiated during filling, whilst fracture originating in the cervical portion is likely caused by occlusal loads.

Keywords: canal taper, compaction force, root stress, vertical compaction, vertical root fracture.

Received 8 September 2005; accepted 1 November 2005

Introduction

As early as 1931, it was suggested that root canal treatment was a factor influencing the incidence of vertical root fractures (Arnold 1931). Although case reports have demonstrated that vertical root fractures can occur in nonroot filled teeth (Yang *et al.* 1995), the principal feature associated with vertically fractured roots is prior root canal treatment (Gher *et al.* 1987). Further studies have shown that vertical root fracture occurs most commonly in the buccolingual plane (Pitts & Natkin 1983, Saw & Messer 1995), may be initiated anywhere at or between the apex and the crown (Pitts & Natkin 1983), and is responsible for 4.3% of endodontic failures (Vire 1991). Attempts have been made to treat these fractures (Friedman *et al.* 1993, Selden 1996, Dederich 1999, Schwartz *et al.* 1999, Hayashi *et al.* 2002, Kawai & Masaka 2002), but a favourable long-term prognosis has yet to be achieved because of complexities associated with material biocompatibility and poor capacity of the restorative materials to achieve radicular resistance to refracture. Since vertical root fractures extend from the root canal to the periodontium, profound and rapid destruction of the bone and periodontium occur in a linear fashion adjacent to the fracture (Harrington 1979). The destruction is a manifestation of debris, necrotic tissue and bacteria harboured in the fracture which prevent

Correspondence: Antheunis Versluis, Minnesota Dental Research Center for Biomaterials and Biomechanics, University of Minnesota, 16-212 Moos Tower, 515 Delaware St SE, Minneapolis, MN 55455, USA (Tel.: +1 612 626 3962; fax: +1 612 626 1484; e-mail: antheun@umn.edu).

repair, thus requiring extraction of the fractured root or entire tooth (Walton *et al.* 1984).

The influence of prior root canal treatment on propensity for vertical root fracture has been examined in several studies. It has been reported that excessive force during lateral compaction caused 84% of vertical root fractures with documentation of many patients experiencing a sound at the time of filling indicative of the root being fractured (Meister *et al.* 1980). Additionally, vertical root fractures have been shown to occur with spreader loads as small as 1.5 kgf (14.7 N) (Holcomb *et al.* 1987). In contrast, another investigation showed the mean load required to cause vertical root fracture was five to six times higher than the load used to fill a canal, casting doubt on the likelihood of fracture occurring at the time of filling (Saw & Messer 1995). It has been postulated that dentine may have sufficient elasticity to permit some separation of root segments without creating a complete fracture, manifesting in small, incomplete fractures created at the time of filling which may eventually become complete vertical root fractures upon extending completely to the periodontium (Walton *et al.* 1984). It is also possible that distortions are stored in dentine and remain quiescent over time. With additional stress applied through mastication or restoration, the latent fractures could occur as complete fractures at a later time (Dang & Walton 1989). Harvey *et al.* (1981) demonstrated that strain increased in the canal wall during compaction, but the photoelastic models used in their study returned to their original unstressed states after filling was completed, casting doubt on the likelihood that stresses were stored. Dang & Walton (1989) noted that it has not been established whether fractures occur at the time of filling or manifest themselves at a later time. At present, this fundamental question remains a point of contention because vertical root fracture is a complex issue that is difficult to study comprehensively.

One of the potential factors which may influence propensity for vertical root fractures is the prepared canal diameter. Generally, taper should be sufficient to permit deep penetration of spreaders or pluggers during filling but should not be excessive to the point where procedural errors occur, and the root is unnecessarily weakened (Walton & Torabinehad 1996). Holcomb *et al.* (1987) remarked that there must be a point at which increased canal width and taper begin to weaken the root. Intuitively, it is reasonable to speculate that increasing the taper of the canal preparation by removing more dentine from the canal wall would diminish the structural integrity of the root. Using finite-element analysis, Ricks-Williamson *et al.* (1995) found the magnitude of generated radicular stresses to be directly correlated with the simulated canal diameters. Wilcox *et al.* (1997) found that root surface craze lines formed on roots where greater percentages of the canal wall were removed. Conversely, it has been reported that no significant correlation exists between fracture load and size of the root, size of the prepared canal, width of the canal walls after instrumentation, and taper of the root or of the canal (Pitts *et al.* 1983). Additionally, greater flaring allows compaction forces to be delivered more effectively to the apical third of the canal and imparts better stress distribution (Harvey *et al.* 1981).

This investigation was designed to evaluate the effect of different canal tapers on radicular stress distributions in an effort to determine whether using instruments of large taper will predispose a root to vertical fracture. The stress distributions were determined utilizing finite element analysis. Given differing opinions relative to whether vertical root fractures occur at the time of filling or at a later time, this study examined stress distributions during vertical compaction of gutta-percha at multiple filling increments and post-filling with the addition of occlusal load.

Materials and methods

Three finite element models of a root filled premolar tooth were created in this study varying only in canal taper. All other aspects of the models were held constant including crown and external radicular morphology, boundary conditions, material properties, compaction forces during filling, and magnitude/direction of applied occlusal load. The tooth model was created by digitizing the external surface of an extracted human mandibular second premolar with a straight root using a white-light optical scanner (Comet 100, Steinbichler Optical Technologies, Neubeuern, Germany) in combination with custom software (Cumulus software, copyright Regents of the University of Minnesota) (Fig. 1a). A straight root was chosen for this canal taper study to eliminate effects due to canal curvature.

Other locally developed software was developed to create internal interfaces (dentine–enamel junction and pulp) based on regular dental anatomy and to add a 200 μm thick periodontal ligament (PDL) layer and a surrounding bone volume to support the root. Cementum and sealer were not modelled separately and were considered to be incorporated in the root dentine and

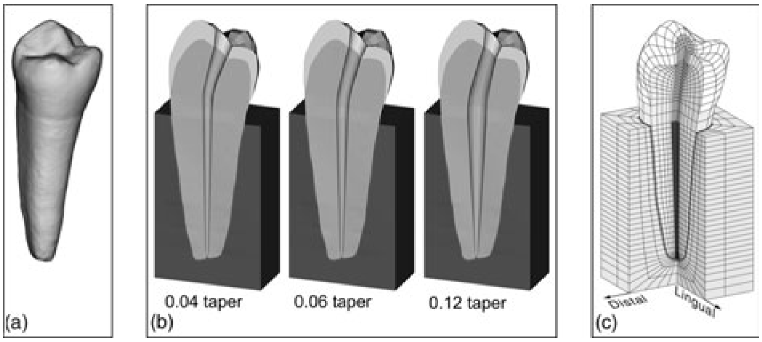

Figure 1 Mandibular second premolar: (a) digitized outer surface, (b) prepared straight root canals for three taper sizes (0.04, 0.06 and 0.12) and (c) three-quarter view of the finite element model for the 0.06 taper, consisting of enamel, dentine, periodontal ligament, bone, gutta-percha and composite.

Table 1 Material properties applied in the stress analysis

Material	Elastic modulus (GPa)	Reference	Poisson's ratio	Reference
Enamel (principal direction)	84	Craig & Powers (2002)	0.33	Farah *et al.* (1989)
Enamel (transverse plane)	42			
Dentine	14.7	Sano *et al.* (1994)	0.31	Farah *et al.* (1989)
Periodontal ligament	0.00118	Dyment & Synge (1935)	0.50	
Bone	0.49	Moroi *et al.* (1993)	0.30	Farah *et al.* (1989)
Gutta-percha	Temperature dependent, see Fig. 3		0.30 (0 °C) 0.35 (30 °C) 0.40 (60 °C)	
Restorative composite	14	Willems *et al.* (1992)	0.24	Craig & Powers (2002)

gutta-percha, respectively. Subsequently, a standard access opening was made in the crown, and root canals were created that represented 0.04, 0.06 and 0.12 mm mm^{-1} tapers (Fig. 1b). The 0.04 and 0.06 tapers were chosen for clinical relevancy, as these are incorporated into commonly used nickel–titanium rotary files and are representative of clinically imparted tapers on the canal space. The drastic 0.12 tapered canal preparation was chosen arbitrarily to simulate the effects of excessive canal preparation. All models were created with a final apical preparation of 0.35 mm at the point of constriction, 0.5 mm from what would be clinically perceived as the radiographic apex. The canal diameter beyond the apical constriction was 0.15 mm. All canal preparations were straight and circular. Subsequently, the custom developed programme generated finite element meshes within the complete geometrical model, the gutta-percha inside the root canal, and a composite restoration in the access opening using quadrilateral element types (Fig. 1c).

Anisotropic properties were applied to the enamel with the principal axis directed perpendicular to the dentine–enamel junction (transverse isotropic). This corresponds to the approximate direction of the enamel rods. Isotropic properties were applied for the dentine, PDL, supporting bone volume, gutta-percha and restorative composite. The PDL was modelled as a soft incompressible connective layer. The applied material properties are summarized in Table 1. The composite shrinkage value due to polymerization shrinkage was selected 0.15% (linear shrinkage), which corresponds with a typical post-gel shrinkage value for a restorative composite. Temperature dependent elastic–plastic gutta-percha properties were applied to simulate warm compaction. Each gutta-percha brand has a different stress–strain curve (Friedman *et al.* 1975, 1977). For this analysis, true stress–strain curves were approximated from the available data in the literature for an average gutta-percha response (Fig. 2). Note that elastic modulus, Poisson's ratio, yield stress and strain hardening were all dependent on the temperature. The coefficient of thermal expansion was 55×10^{-6}/°C (Price 1918). An arbitary range of friction coefficients (0.10–0.25) were evaluated to account for the friction between the gutta-percha and the root canal wall.

The development of radicular stresses was analysed during three consecutive filling steps as well as for an occlusal load after the root filling using finite element

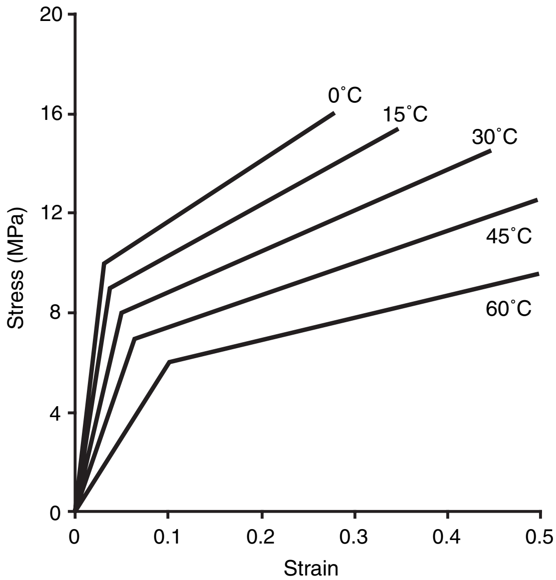

Figure 2 Approximated temperature-dependent uniaxial true stress–strain curves for gutta-percha, applied in the analysis.

analysis (MSC.Marc, MSC.Software Corporation, Santa Ana, CA, USA). Warm gutta-percha was compacted in three separate vertical increments until the canal was filled (Fig. 3a–d). The gutta-percha temperature at the start of compaction was 60 °C and was gradually cooled down during the filling procedure until it reached 37 °C. In this analysis, two vertical compaction forces were tested at 10 and 15 N, as compaction forces ranging from 10 to 30 N have been reported in the literature (Harvey *et al.* 1981). The forces were applied by means of a simulated plugger (Fig. 3b–d). The plugger surface had slightly rounded edges and a tip-diameter that was 0.5 mm smaller than the canal diameter at each compaction increment. Only 2 mm of plugger tip was modelled and was considered rigid in comparison with the gutta-percha. In other words, the plugger tip was considered undeformable.

After complete filling, the access space was closed using a simulated bonded restorative composite. The effects of the polymerization reaction were represented by the associated shrinkage. After the composite was placed and cured, a 50 N occlusal load was applied in the buccolingual plane to the triangular ridge of the buccal cusp at an angle of 60° with the vertical axis (Fig. 3e). The value of the occlusal force was chosen to represent a relatively high biting force. During the analysis, the root was supported by the surrounding bone volume via the soft PDL layer, which was given incompressible properties to approximate fluid behaviour. To simulate proximal constraints and provide model stability, the buccal, lingual and apical surfaces of the bone volume were fixed in buccal, lingual and apical directions, respectively.

Equivalent, circumferential and radial stress distributions in the filled root were collected. Equivalent stresses are stresses that represent the three-dimensional stress condition with a single value according to a certain criterion, in this case the modified von Mises criterion (Versluis *et al.* 1997). This criterion is based on the well-known von Mises criterion, but it is modified to take the difference between compressive and tensile strength into account that many dental materials and hard tissues exhibit. For example, dentine is about three times stronger in compression than tension (Craig & Powers 2002). Equivalent stresses are useful to visualize and evaluate multi-axial stress distributions. Circumferential stresses are stresses tangential to the root canal wall in the horizontal plane. These stresses may cause vertical fractures along the root canal. Radial stresses are stresses perpendicular to the canal wall in the horizontal plane. Radial stresses correspond with the pressure applied on the root canal surface through the gutta-percha by the plugger during compaction.

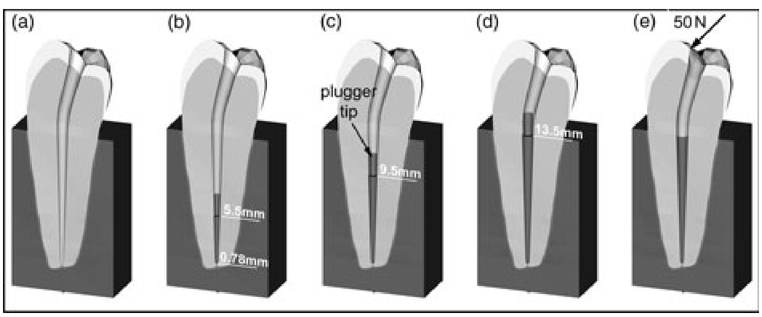

Figure 3 Vertical condensation modelling steps: (a) preparation; (b–d) first, second and third gutta-percha increments, only the plugger tip was modelled; and (e) composite restoration with occlusal loading.

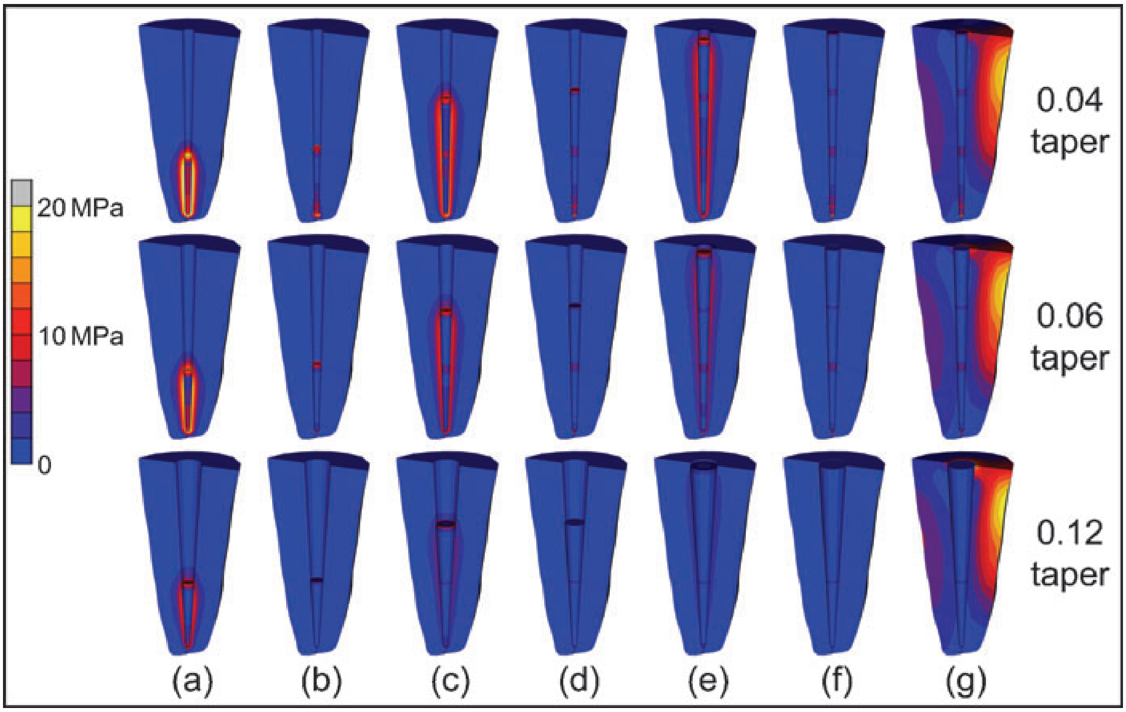

Figure 4 Equivalent stress distributions in a root with three different canal tapers: (a–f) during filling; and (g) followed by a 50 N occlusal loading on the buccal cusp incline. The compaction force was 10 N.

Results

Only the stresses in the root were analysed in this study. The simulation shows that during each vertical compaction increment, stresses are generated in the root along the root canal wall (Fig. 4a–f). The figures demonstrate the distribution of equivalent stresses according to a linear colour scale, where yellow (and white) indicate areas with the highest stresses, and blue the lowest. Note that areas with high stresses are most likely under tension, as the von Mises criterion was modified to create a weighted bias towards tensile stresses. The highest stress levels were obtained during the first filling increment and became lower with each subsequent increment. The stresses tended to be higher closer to the load application (plugger), and gradually decreased along the canal length until they increased again at the apical constriction. After the compaction load was removed, some small residual stresses remained in the apical area depending on the amount of residual elastic deformation of the gutta-percha (Fig. 4b,d,f). The analysis also showed that the stress levels decreased when the taper increased. The stress distribution results for the 10 N compaction force indicated equivalent stresses along the root canal wall in excess of 25 MPa for the 0.04 taper, whilst the 0.06 and 0.12 tapers were in the order of 20 and 11 MPa, respectively.

The stress pattern shifted when an occlusal force was applied to the root filled tooth (Fig. 4g). Instead of observing concentrated stresses along the canal wall as is demonstrated during compaction, the occlusal force generated high (tensile) stresses at the cervical portion of the lingual root surface. The highest equivalent stress values were found for the largest taper and lower values for the smaller tapers (approximately 20, 19 and 18 MPa for the 0.12, 0.06 and 0.04 tapers, respectively).

Examination of the circumferential and radial stress distributions along the root canal wall (Fig. 5) confirms the observations from the equivalent stress patterns. Although the canals were perfectly circular, the stresses around the canals varied due to the asymmetry of the root anatomy. The graphs plot the range of occurring stresses as a band between the minimum and maximum canal surface values calculated at each horizontal cross-section. The highest circumferential and radial stresses were found during compaction of the first gutta-percha increment, whilst an increase in

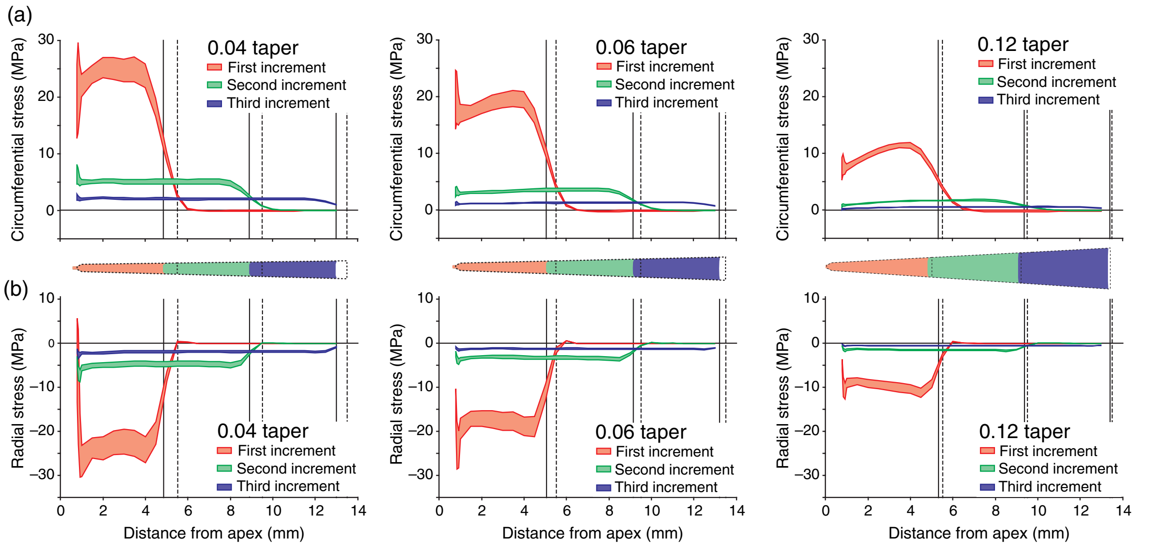

Figure 5 Circumferential (a) and radial (b) stress ranges along the canal wall during three warm vertical compaction increments for three tapers. Vertical lines indicate gutta-percha position before (dashed line) and during 10 N compaction (solid line). Positive values indicate tensile stresses, negative values are compressive.

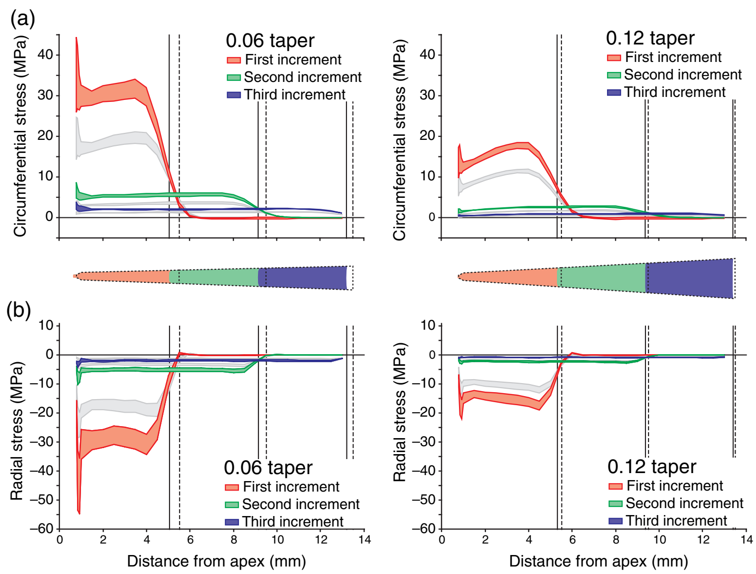

Figure 6 Circumferential (a) and radial (b) stress ranges along the canal wall during three warm vertical compaction increments for two tapers (0.06 and 0.12) with 15 N compaction force. For comparison, the grey data represents the stress range at 10 N compaction force. Vertical lines indicate gutta-percha position before (dashed line) and during compaction at 15 N (solid line).

taper reduced the stress levels for same compaction force. Furthermore, the figures show that the stress peaks at the apical canal constriction generally decreased with increasing taper. In some cases, the apical stress peaks were lower than the stress levels closer to the plugger. Where the equivalent stress did not identify the type of stress, these figures show that the circumferential stresses were predominantly tensile, whilst the radial stresses were compressive. Increasing the compaction force from 10 to 15 N increased the stress levels by about 75% in the 0.06 and 0.12 taper configurations (Fig. 6). The 15 N compaction force turned out to be too high for the 0.04 taper case, and resulted in severe overfilling. The tendency of the stresses to peak at the apical constriction increased with higher compaction loads.

All shown results were determined for a friction coefficient between the gutta-percha and root canal wall of 0.10. Increasing the friction coefficient to 0.25 tended to reduce the stress levels slightly, where the smaller tapers were most affected (up to 5% decrease for the 0.04 taper).

The diameter of the simulated plugger was 0.5 mm smaller than the canal diameter at the top of the gutta-percha increment before compaction (Fig. 3b–d). Applying the compaction force as an evenly distributed load on the top surface of the gutta-percha plug decreased the circumferential stresses close to the load application point by about 5% for the first filling increment (10% for the 15 N compaction force). However, higher peak stresses were found at the apical constriction.

Discussion

Given increasing acceptance of rotary instrumentation as a technique for cleaning and shaping the canal space, it is important to examine the effect of specific tapers imparted by rotary instrumentation of the canal wall as it relates to vertical root fracture. The clinician must make a decision to use instruments which have an inherently larger or smaller taper based on the architecture present in a given canal. Choosing a smaller taper may reduce the risk of procedural accidents and untoward events during cleaning and shaping, but it may compromise the cleanliness of the canal system and placement of filling material. Choosing too large a taper may increase canal cleanliness (especially in the coronal and mid-root areas), but may also increase the potential for strip perforations, other procedural accidents, and may predispose the root to vertical fracture if, indeed, greater reduction of root structure increases stress in the canal wall. Assessment of stress levels by measuring deformation patterns inside the root canal is extremely difficult, leaving investigators with indirect external observations at best. Finite element analyses have therefore been utilized to address these difficulties and gain insight into internal stress distributions (Duret *et al.* 1987, Ricks-Williamson *et al.* 1995, Saw & Messer 1995, Lertchirakarn *et al.* 2003b).

Choice of model definitions

This study used finite element analysis to examine the effect of canal taper on radicular stresses. An important advantage of using a finite element analysis is that all conditions can be kept exactly identical (such as tooth anatomy, mechanical properties, compaction loading, root support, temperature profiles, incremental procedures, etc.), whilst only the taper is varied. This allowed a straightforward comparison of the different tapers. Furthermore, the numerical method ensures that the prepared canals have exactly the specified taper, which could have been more difficult to achieve in a physical experiment where the resulting taper may depend on the width of the original internal diameter. Since stresses are determined by geometrical shape, mechanical properties, loading and constraining conditions, and sometimes loading history, it is important to review the applied model definitions and their potential impact.

For this study, a straight rooted premolar was chosen. A curved canal would have modified the stress distributions, which could have obscured the basic effect of taper size that was the subject of this study. In a recent finite element analysis, Lertchirakarn *et al.* (2003a) reported that canal shape, root shape, and dentine thickness affect tensile stress distributions. They further reported that canal shape was the most important factor, where areas of reduced radius of curvature strongly influenced stress concentrations. They postulated that natural teeth may be subject to even greater stress concentrations as a result of localized irregularities in the canal wall or external tooth structure. As rotary instrumentation typically imparts a round shape to the canal, only circular canals were evaluated here. Other irregularities in the root were not specifically modelled because our objective was to develop a basic understanding of the general stress distribution rather than specific cases. Note that irregular canal shapes would raise stress levels mainly during filling, as occlusal loads are less likely to seriously affect stresses along the canal surface (Fig. 4g).

The applied material properties, the second factor determining the stress, were based on values reported in the literature (Table 1). Anisotropic properties were only applied for the enamel. In contrast to enamel, dentine anisotropy is less well-established. Although the microstructure of dentine is unmistakably anisotropic, its stiffness response has been shown to be isotropic or mildly anisotropic at best (Wang & Weiner 1998, Kinney *et al.* 2004). Probably more significant for the properties definition of dentine was its homogeneous distribution. It has been shown, for example, that the microhardness in coronal dentine varies with depth (Wood *et al.* 2003). However, as there is still insufficient data available about how each tissue property varies through the entire tooth system and considering that those variations are unlikely to change the general conclusions, the decision to apply homogenous distributions for the property values seems prudent. The literature typically reports a wide range of values for the tissues involved, which is a reflection of differences in testing methods and inevitable natural diversity. Since there are thus no universally correct values for tissue properties, the results of this analysis should be considered quantitatively only under the exact applied conditions. Although natural variation is an inherent reality in biomedical research, universal scientific insight in complex interactions transcends specific imperfections.

The third factor determining the radicular stress is the load application (compaction and occlusal) and the external support of the root. The loading is characterized by the way it is delivered and its magnitude. The vertical compaction force was delivered by a simulated plugger with a diameter 0.5 mm smaller than the surrounding canal. The size of the plugger was a factor in the stress distribution along the canal wall because applying the compaction force by a perfectly fitting plugger (simulated by an evenly distributed compaction force) slightly lowered the circumferential stresses along the canal wall, whilst it increased the stresses at the apical constriction. Magnitudes for lateral compaction forces have been reported up to 30 N ($\sim$3 kgf) (Harvey *et al.* 1981). However, when forces higher than 10 N were applied for the smaller tapers, the gutta-percha was squeezed through the apical constriction. Even 15 N turned out to be too high for the 0.04 taper size. Furthermore, the ultimate tensile strength of dentine (94–106 MPa, Sano *et al.* 1994) would have been approached for the smaller tapers with a 30 N vertical compaction force. These observations suggest that taper size dictates the maximum compaction force that should be applied. To create consistent load conditions, a 10 N baseline compaction force was chosen for all tapers in the analysis. In addition to the compaction forces, a 50 N occlusal load was applied after the simulated root canal treatment for the comparison of the stress distributions in a root filled tooth. Although this masticatory load only represented one possible load case, the general bending effects it introduced in the root can be considered representative for a significant masticatory event whilst the way stresses distributed in the root was indicative for higher as well as lower load values.

The root was supported through a flexible connective layer simulating the PDL and a surrounding bone volume. The analysis indicated that during compaction, radicular stresses were concentrated along the root canal and were minimally affected by the external support (Fig. 4a–f). Therefore, the exact modelling of PDL and supporting bone structure was probably less critical during the filling simulation. During an occlusal loading, however, the radicular stress distribution was strongly affected by the response of the supporting periodontium and surrounding bone. Despite the admittedly simplistic modelling of the extremely complex and still not well-understood PDL tissues, the stress conditions induced in the root during the occlusal load appear as anticipated theoretically. The occlusal load on the buccal cusp generated bending conditions in the tooth. During bending, maximum stresses are expected at the outer surfaces of the bent structure, whilst stress levels around the centre should be low. In this analysis, the highest stresses were indeed found at the lingual and buccal root surfaces (tensile and compressive stresses, respectively) (Fig. 4g). Note that the buccolingual plane has been indicated as the location where vertical root fracture most commonly occurred (Pitts & Natkin 1983, Gher *et al.* 1987, Saw & Messer 1995).

The last factor that may play a role in the resultant radicular stress distribution is the load and deformation history. This study indicated that some residual stress may remain in the root structure subsequent to warm vertical compaction of gutta-percha (Fig. 4b,d,f). The amount of residual stresses depended on the physical properties of the gutta-percha and root dentine and on the amount of deformation. The smallest taper, which generated the highest radicular stresses during filling, showed the highest residual stresses. Dang & Walton (1989) commented about the possibility that distortions are stored in dentine and remain quiescent for life. With additional stress applied through restoration or mastication, these latent fractures could manifest themselves as complete fractures months or years later. However, it is unlikely that the low residual stress levels determined in our analysis would be stored for very long considering the viscoelastic nature of dentine. Harvey *et al.* (1981) conducted a photoelastic study and concluded that photoelastic models returned to their original unstressed states after lateral compaction was complete. Even if residual stresses would linger, they concentrated near the apical constriction and were hardly involved in the stress distribution that ensued from the occlusal load. Therefore, the current study does not support a significant role for residual stresses from filling in root fracture for the conditions modelled in this analysis.

Effect of taper on radicular stresses

The results of the simulated vertical compaction of warm gutta-percha indicated that, given the same compaction force, radicular stresses decreased with increasing taper (Fig. 4a–f). This intuitively unexpected conclusion can be explained by the fact that increasing taper results in larger contact surface areas which helps to spread out the compaction force and, thus, lowers the level of transferred stresses (Fig. 5b). The analysis also indicated that the stresses were generally higher in the areas near the plugger tip, whilst the resultant stress levels decreased with each subsequent gutta-percha increment. The latter can also be attributed to the increased contact surface area available to each subsequent gutta-percha increment for better distribution of the compaction force. Two other factors that played a role in the transfer of compaction forces into the root were the taper-angle and the friction. Relative to taper-angle, a smaller taper constitutes a less constrictive canal, causing more of the force to be transferred lower in the increment (Fig. 5). Friction resists the tendency for the gutta-percha plug to be pushed down the root canal, and therefore tends to transfer the compaction force higher in the increment, which lessens the general stress level due to the larger surface area. The analysis indicated up to 5% reduction in radicular stresses when the coefficient of friction was increased from 0.10 to 0.25. Actual friction coefficient data for the gutta-percha were not available, but it may be expected that friction under clinical conditions will be smaller rather than higher due to the presence of sealer.

The conclusion that larger tapers resulted in reduced radicular stress levels during compaction is corroborated by other investigators that studied lateral compaction. Harvey *et al.* (1981) reported that a tapered canal imparts better stress distribution than an untapered canal. Holcomb *et al.* (1987) reported that the wider the root, the wider the root canal, and the wider the root canal in relation to the root width, the more resistant the root was to fracture at higher spreader load values. However, Ricks-Williamson *et al.* (1995), using finite element analysis, found that the magnitudes of generated stresses during compaction increased with increased canal diameter. This contrasting conclusion could be the result of their model definition, which may have allowed tensile stress generation between the gutta-percha, canal wall, and finger plugger. Nevertheless, it seems intuitive to expect higher root stresses for larger canal diameters because it reduces the amount of dentine and, thus, structural integrity. However, the stress situation is more complex than it may appear because stress is determined by multiple factors. Figure 7 shows that, given the same total internal load, very small canal diameters generate higher stresses along the canal wall because there is less surface area to spread the filling force. On the other extreme, very large canal diameters lead to higher stress levels due to the decreasing wall thickness and thus lower wall stiffness. In other words, the resultant stress distribution is determined by how the filling force is spread over the internal surface area and by the stiffness of the remaining wall thickness. Note that if a constant pressure (i.e. load/area) is applied to the canal wall instead of a constant load (i.e. pressure × area), the stress levels will always increase with any increase in canal diameter, because the total applied load increases due to the increased area and the wall stiffness decreases due to the thinner walls. Complex interactions can deceive intuition. Numerical methods are well-suited for interrogating complicated interactions and are, therefore, indispensable for the study of radicular stresses.

Effect of taper on vertical root fracture

Stresses in root filled roots are a persistent concern because they are believed to play a critical role in root fracture (Lertchirakarn *et al.* 2003a). Although fracture is ascribed to radicular stresses, there is no consensus about where and when vertical root fracture is initiated. Saw & Messer (1995) found fracture lines confined primarily to the apical portion of the root and suggested that vertical root fracture begins in the apical portion of the root and propagates coronally. Harvey *et al.* (1981) also reported that stresses were localized in the apical third of the root, and moved coronally as the canal was filled. In contrast, Dang & Walton (1989) suggested that most vertical root fractures occurred in the middle third of the root. These different observations are not necessarily conflicting because they could indicate that there are multiple mechanisms involved in root fracture. Two important principles for radicular stress distributions during filling are illustrated by Fig. 7: (a) root stresses generated from inside the root canal are always the highest at the canal wall; and (b) thinner walls increase the average stress level in the wall. If the whole root would have the same strength throughout, the most likely fracture mechanism during filling would be a crack that initiates at the canal wall surface because that is where the ultimate stress will be exceeded first. However, as strength properties may

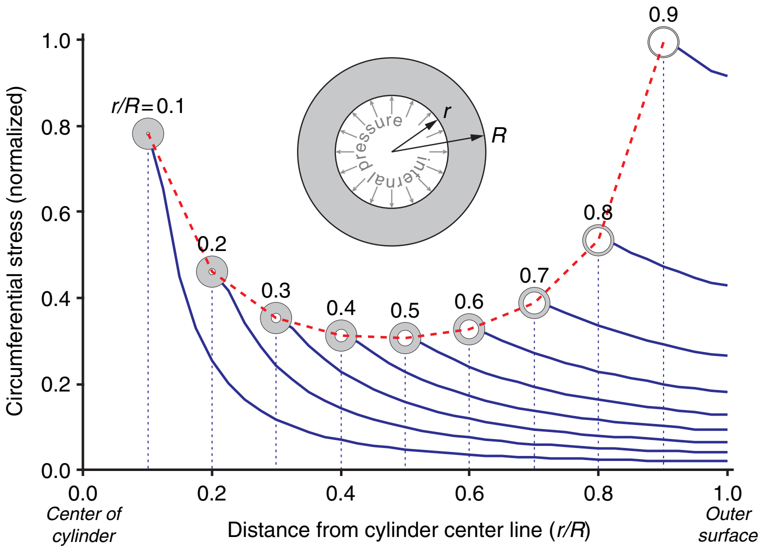

Figure 7 Circumferential stress distribution in cylinder wall due to internal pressure for a range of canal diameters. Total applied load (pressure × internal wall surface) is constant. The dashed curve connects the maximum circumferential stress values, which occurred at the internal wall.

vary throughout the root, and the root structure may contain additional local stress raising irregularities, an elevated general stress level may predispose a root to fracture in other areas as well. Wilcox *et al.* (1997) reported an increase in spreader-induced vertical root fractures associated with increases in canal enlargement. In their study, they increased the canal width successively from 20% to 50% (corresponding with r/R-ratio from 0.2 to 0.5), which, according to Fig. 7, could have reduced the stress peak at the canal wall and tripled the general stress level closer to the root surface where craze lines may have been more likely to exist and develop into cracks. Note that lateral compaction adds an asymmetrical loading component on the canal wall in addition to the more even distribution during vertical compaction. These lateral components could introduce bending conditions in the root, potentially increasing the general stress levels in the middle or coronal third of the root. Nevertheless, except for extreme cases with very high asymmetrical loads, the general principle applies that if a canal is stressed from the inside, the highest stresses will be generated at the canal wall.

Another point of contention is when vertical root fracture is initiated: during the filling process or during subsequent functioning of the root filled tooth. This issue might be closely related to the debate about where fracture is initiated. The stress distributions derived in this study suggest that both cases stress different areas of the root: vertical compaction forces induce stresses that are concentrated around the root canal (Fig. 4a–f), whilst occlusal loads tend to introduce bending conditions in the tooth generating stresses that concentrate at the external (buccal and lingual) root surfaces (Fig. 4g). Therefore, according to the specific conditions simulated in this analysis, fractures that originate at the canal wall surface and in the apical section are most likely caused by the filling process, whilst fractures that originate at the external surface of the root are most likely propagated by functional coronal loading. It is interesting to note, that based solely on the vertical rather than horizontal nature of the tensile stress distributions during tooth bending conditions, the analysis implies a horizontal rather than vertical root fracture mechanism. If functional loading is involved in vertical root fractures, it is conceivable that it occurs through a process that propagates existing vertical defects, such as craze lines. It is important to re-emphasize that the stress analysis did not consider individual irregularities such as craze lines or dynamic stress distributions that typically take place during fracture propagation (e.g. during a fatigue process). Such clinical realities could raise stress levels in the root locally beyond the values calculated in the analysis.

Clinical implications

The mechanism of vertical root fracture is still not fully understood. However, it is widely accepted that stresses in the canal wall play a critical role. The current study shows that understanding the implications of canal taper as they relate to radicular stresses requires a careful consideration of multiple factors. Clinical decisions regarding taper must foremost be made within the context of maximizing canal cleanliness and adherence to fundamentally sound principles to rid the canal system of pathogens and their byproducts. However, even though more advantageous stress distributions during filling with large tapers has been shown, indiscriminate decisions to impart a larger taper on the canal than clinically necessary should be considered ill-advised. Filling forces occur only during the root canal treatment and are easily controlled by a discerning professional. Masticatory loads, on the contrary, are recurrent and cannot practically be controlled. Preservation of dental hard tissue remains thus well-advised for maintaining overall structural integrity and minimizing predisposition to vertical root fracture after root canal treatment. During filling, the risk of initiating fracture can be reduced by understanding the effect of canal taper size on radicular stresses. It was shown that small canal tapers are more likely to generate high stresses in the apical third during compaction, especially during the first gutta-percha increment. Comparison of stress levels during filling and functional occlusal loading suggests that during vertical compaction of the first gutta-percha increment, internal stresses may exceed the stress levels caused by a relatively high functional load (50 N). These filling stresses increased rapidly at the apical constriction if the compaction forces were increased (Fig. 6). Awareness of these dynamics should remind the practitioner not to exceed the necessary compaction forces, especially in a first (vertical) increment, to reduce the risk of exceeding the apical fracture properties of the root.

Conclusions

(1) During filling, root stress decreases as the canal taper increases, with generated stresses being greatest at the apex and along the canal wall.
(2) After root filling is complete and occlusal force is applied, the relationship is reversed. The generated stress is greatest at the cervical portion of the root surface, and increases slightly as taper increases.
(3) It is likely that vertical root fractures initiated at the apex are a result of filling forces, whereas vertical root fractures initiated cervically are a manifestation of subsequent masticatory events on the root filled tooth.

Acknowledgements

This study was supported in part by the Minnesota Dental Research Center for Biomaterials and Biomechanics. Ms Maria R. Pintado generously contributed the digitized premolar external anatomy used in this analysis ('A Digital Environment for Teaching Oral Anatomy – A Student-Oriented Approach', 2004). The authors also thank Dr D. Tantbirojn for her input.

References

Arnold LH (1931) Discussion. *Journal of the American Dental Association* **18**, 483.
Craig RG, Powers JM (2002) *Restorative Dental Materials*, 11th edn. St Louis, MO: Mosby.
Dang DA, Walton RE (1989) Vertical root fracture and root distortion: Effect of spreader design. *Journal of Endodontics* **15**, 294–301.
Dederich DN (1999) CO_2 laser fusion of a vertical root fracture. *Journal of the American Dental Association* **130**, 1195–9.
Duret B, Duret F, Reynaud M (1987) Long-life physical property preservation and postendodontic rehabilitation with the composipost. *Compendium* **17**(Suppl. 20), S50–S56.
Dyment MI, Synge JL (1935) The elasticity of the periodontal membrane. *Oral Health* **25**, 105–9.
Farah JW, Craig RG, Meroueh KA (1989) Finite element analysis of three- and four-unit bridges. *Journal of Oral Rehabilitation* **16**, 603–11.
Friedman CM, Sandrik JL, Heuer MA, Rapp GW (1975) Composition and mechanical properties of gutta-percha endodontic points. *Journal of Dental Research* **54**, 921–5.
Friedman CE, Sandrik JL, Heuer MA, Rapp GW (1977) Composition and physical properties of gutta-percha endodontic filling materials. *Journal of Endodontics* **3**, 304–8.
Friedman S, Moshonov J, Trope M (1993) Resistance to fracture of roots, previously fractured and bonded with glass ionomer cement, composite resin and cyanoacrylate cement. *Endodontics and Dental Traumatology* **9**, 101–5.
Gher ME Jr, Dunlap RM, Anderson MH, Kuhl LV (1987) Clinical survey of fractured teeth. *Journal of the American Dental Association* **114**, 174–7.
Harrington GW (1979) The perio-endo question: differential diagnosis. *Dental Clinics of North America* **23**, 673–90.
Harvey TE, White JT, Leeb IJ (1981) Lateral condensation stress in root canals. *Journal of Endodontics* **7**, 151–5.
Hayashi M, Kinomoto Y, Miura M, Sato L, Takashige F, Ebisu S (2002) Short-term evaluation of vertically fractured roots reconstructed with dentin-bonded resin. *Journal of Endodontics* **28**, 120–4.
Holcomb Q, Pitts DL, Nichols JI (1987) Further investigation of spreader loads required to cause vertical root fracture during lateral condensation. *Journal of Endodontics* **13**, 277–84.
Kawai K, Masaka N (2002) Vertical root fracture treated by bonding fragments and rotational replantation. *Dental Traumatology* **18**, 42–5.

Kinney JH, Balooch M, Marshall GW, Marshall SJ (2004) A micromechanics model of the elastic properties of human dentine. *Archives of Oral Biology* **44**, 813–22.

Lertchirakarn V, Palamara JEA, Messer HH (2003a) Patterns of vertical root fracture: Factors affecting stress distribution in the root canal. *Journal of Endodontics* **29**, 523–8.

Lertchirakarn V, Palamara JEA, Messer HH (2003b) Finite element analysis and strain-gauge studies of vertical root fracture. *Journal of Endodontics* **29**, 529–34.

Meister Jr F., Lommel TJ, Gerstein H (1980) Diagnosis and possible causes of vertical root fractures. *Oral Surgery, Oral Medicine, and Oral Pathology* **49**, 243–53.

Moroi HH, Okimoto K, Moroi R, Terada Y (1993) Numeric approach to the biomechanical analysis of thermal effects in coated implants. *International Journal of Prosthodontics* **6**, 564–72.

Pitts DL, Natkin E (1983) Diagnosis and treatment of vertical root fractures. *Journal of Endodontics* **9**, 338–46.

Pitts DL, Matheny JE, Nicholls JI (1983) An *in vitro* study of spreader loads required to cause vertical root fracture during lateral condensation. *Journal of Endodontics* **9**, 544–50.

Price WA (1918) Report of laboratory investigations on the physical properties of root filling materials and the efficiency of root fillings for blocking infection from sterile tooth structures. *National Dental Association Journal* **5**, 1260–80.

Ricks-Williamson LJ, Fotos PG, Goel VK, Spivey JD, Rivera EM, Khera SC (1995) A three-dimensional finite-element stress analysis of an endodontically prepared maxillary incisor. *Journal of Endodontics* **21**, 362–7.

Sano H, Ciucchi B, Matthews WG, Pashley DH (1994) Tensile properties of mineralized and demineralized human and bovine dentin. *Journal of Dental Research* **73**, 1205–11.

Saw LH, Messer HH (1995) Root strains associated with different obturation techniques. *Journal of Endodontics* **21**, 314–20.

Schwartz RS, Mauger M, Clement DJ, Walker WA III (1999) Mineral trioxide aggregate: a new material for endodontics. *Journal of the American Dental Association* **130**, 967–75.

Selden HS (1996) Repair of incomplete vertical root fracture in endodontically treated teeth – *in vivo* trials. *Journal of Endodontics* **22**, 426–9.

Versluis A, Tantbirojn D, Douglas WH (1997) Why do shear bond tests pull out dentin? *Journal of Dental Research* **76**, 1298–307.

Vire DE (1991) Failure of endodontically treated teeth: classification and evaluation. *Journal of Endodontics* **17**, 338–42.

Walton RE, Torabinehad M (1996) *Principles and Practice of Endodontics*, 2nd edn. Philadelphia, PA: WB Saunders Co., p. 204.

Walton RE, Michelich RJ, Smith GN (1984) The histopathogenesis of vertical root fractures. *Journal of Endodontics* **10**, 48–56.

Wang R, Weiner S (1998) Human root dentin: Structural anisotropy and Vickers microhardness isotropy. *Connective Tissue Research* **39**, 269–79.

Wilcox LR, Roskelley C, Sutton T (1997) The relationship of root canal enlargement to finger-spreader induced vertical root fracture. *Journal of Endodontics* **23**, 533–4.

Willems G, Lambrechts P, Braem M, Celis JP, Vanherle G (1992) A classification of dental composites according to their morphological and mechanical characteristics. *Dental Materials* **8**, 310–9.

Wood JD, Wang R, Weiner S, Pashley DH (2003) Mapping of tooth deformation caused by moisture change using moire interferometry. *Dental Materials* **19**, 159–66.

Yang SF, Rivera EM, Walton RE (1995) Vertical root fracture in non-endodontically treated teeth. *Journal of Endodontics* **21**, 337–9.